NOTES AND CORRESPONDENCE

Statistical Detection of Anomalous Propagation in Radar Reflectivity Patterns

STANISLAW MOSZKOWICZ

Aerology Division, Institute of Meteorology and Water Management, Legionowo, Poland

GRZEGORZ J. CIACH AND WITOLD F. KRAJEWSKI

Iowa Institute of Hydraulic Research, University of Iowa, Iowa City, Iowa

19 January 1993 and 16 November 1993

ABSTRACT

The problem of anomalous propagation (AP) echoes in weather radar observations has become especially important now that rainfall data from fully automatic radar systems are sometimes applied in operational hydrology. Reliable automatic detection and suppression of AP echoes is one of the crucial problems in this area.

This study presents characteristics of AP patterns and the initial results of applying a statistical pattern classification method for recognition and rejection of such echoes. A classical radar (MRL-5) station operates in central Poland performing volume scanning every 10 min. Two months of hourly data (June and September of 1991) were chosen to create learning and verification samples for the AP detection algorithm. Each observation was thoroughly analyzed by an experienced radar meteorologist. The features taken into account were visually estimated local texture and overall morphology of echo pattern, vertical echo structure, time evolution (using animation), and the general synoptic information. For each 4 km × 4 km pixel of 933 observations the human classification was recorded resulting in a sample of 631 166 points with recognized echo type, 14.6% of them being AP echoes. The unsuppressed AP echo impact on monthly accumulated precipitation was 59% of the actual sum for the month of June and as much as 97% for September.

Three Bayesian discrimination functions were investigated. They differ in selection of the feature vector. This vector consisted of various local radar echo parameters: for example, maximum reflectivity, echo top, and horizontal gradients. The coefficients of the functions were calibrated using the June sample. The AP echo recognition error was about 6% for the best-performing function, when applied to an independent (September) sample, which would make the method acceptable for operational use.

1. Introduction

Automatic detection of anomalous propagation (AP) patterns in radar echoes is perhaps the single most important issue hampering operational use of quantitative radar rainfall estimates in real-time hydrologic forecasting. Failure to recognize and eliminate anomalous propagation echoes from further processing in rainfall estimation could lead to erroneous accumulations that might trigger fictitious floods. An inevitable consequence of this would be lowered public credibility of the flood warning and forecasting system. Therefore, fully automated radar rainfall estimation systems must include an elaborate data quality component to minimize the risk of false alarms. Anomalous propagation echo detection is an essential element of that component.

While there are many possible approaches to the problem none seems to be clearly superior. Use of complementary satellite information on cloudiness, and therefore on the potential for rainfall occurrence, was demonstrated to be useful by Fiore et al. (1986). Other possibilities depend on the technical capabilities of the radar in use. For example, radars equipped with a Doppler information processor may analyze the dynamic properties of the echoes in question (Doviak and Zrnić 1984). Hamuzu and Wakabayashi (1991) proposed a ground clutter filtering method based on real-time analysis of time correlation of the radar signal. However, many existing radar systems with the limited capabilities of performing only reflectivity measurements at a single wavelength and polarization must rely on echo pattern analysis methods. Also, proper climatological utilization of existing collections of conventional radar data requires prior removal of anomalous propagation clutter contaminating them.

In this paper we present a statistical approach to the problem of AP echo detection in radar reflectivity data,

Corresponding author address: Dr. Witold F. Krajewski, Iowa Institute of Hydraulic Research, 404 Hydraulics Lab, University of Iowa, Iowa City, IA 52242.
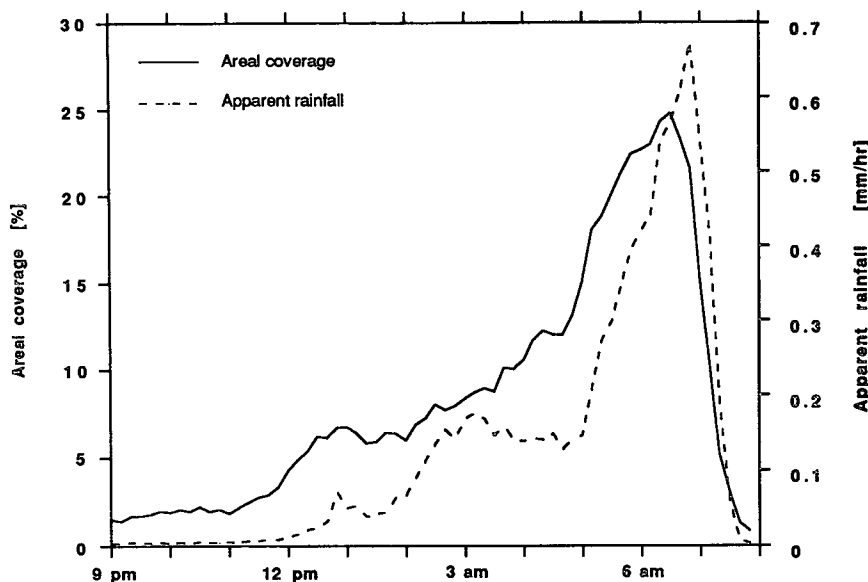
FIG. 1. Time evolution of the areal coverage by AP echoes caused by radiative inversion for the night of 9/10 June 1991. The dashed line corresponds to the same data interpreted as space-averaged apparent rainfall, calculated using the Marshall–Palmer Z–R conversion (the averaging was carried over the entire observation area). The radar observations were performed every 10 min.

based on linear discrimination functions. Its effectiveness was evaluated by comparisons made with results obtained by a human expert. The main goal of this paper is to formulate the method and to present our experimental framework for its systematic calibration (estimation of the parameters) and validation, whereas the results reported here are of preliminary nature.

The paper is organized as follows. In the next section we briefly present general properties of anomalous propagation echoes in central Poland. This is followed by a short description of the preparation of the calibration and verification data sample that is the basis of our results. Next we present formulation of a statistical model for false echo detection and describe its implementation in our situation. The results of the method's evaluation are followed by the conclusions and recommendations section.

2. Characteristics of AP echoes in Poland

Anomalous propagation ground clutter appears when the radar ray path curvature in the surface layer of troposphere is greater than the curvature of the earth's surface. It occurs when vertical radio refractivity gradient in this layer is less than -157 km^{-1} (superrefraction), which causes the radar waves to be trapped in this layer (Bean and Dutton 1968). This results in strong echoes from the earth's surface even for distances of hundreds of kilometers. The phenomenon is very complex and depends not only on the refraction conditions, but also on the length and polarization of the

electromagnetic waves (Ko 1985). Meteorological conditions leading to anomalous propagation echoes typically occur when a temperature inversion in the atmospheric surface layer is concurrent with a sharp vertical decrease of the specific humidity. Four common types of temperature inversions associated with anomalous propagation are described by Battan (1973).

In central Poland, anomalous propagation occurs mainly as a result of nocturnal radiative cooling. In addition, there are a very few cases of rather weak and short-lived AP echoes during daylight, typically caused by the "after storm" superrefraction. Analysis of June data shows that radiation-caused AP echoes appear about 2 h before sunset and disappear about 3 h after sunrise; in September the respective numbers are 40 min, and 2 h. Figure 1 shows the time evolution of the areal coverage by radar echoes and the space-averaged apparent rainfall, calculated based on the Marshall–Palmer Z–R relationship, for an example of the superrefraction case during the night of 9/10 June 1991. The evolution features a characteristic slow increase of both parameters, beginning before sunset and reaching maximum about 2–3 h after sunrise, and a very rapid decay of the echo during the half hour that follows.

More general characteristics of AP echoes in Poland were prepared based on the two-month sample of manually classified observations that is described in the next section. They are expressed in terms of the percentage of observed nonzero radar echo points that were recognized as AP echoes. We call it hereafter a
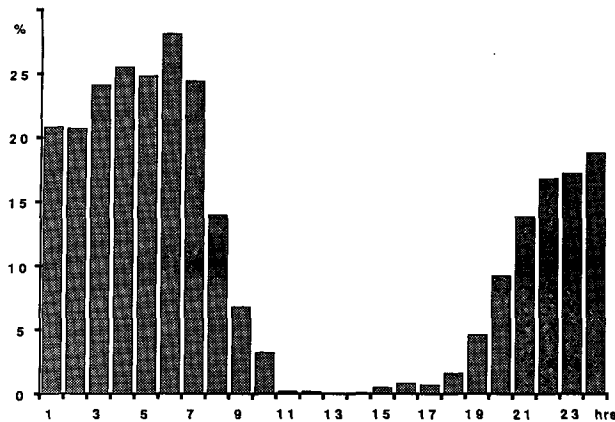
FIG. 2. Diurnal dependence of the spatially averaged conditional probability of AP echoes for the two-month sample of manually classified observations.

conditional probability of AP (conditioned on the occurrence of nonzero echo). The time dependence of the AP echo conditional probability is presented in Fig. 2. One can see that in the middle of a day it is negligible, whereas just after the sunrise more than 25% of observed echoes are anomalous propagation clutters. Figure 3a shows the spatial distribution map of the conditional probability of AP. The field is highly nonhomogenous and reflects quite well the peculiarities of orography in central Poland. For comparison, the probability map of meteorological echo occurrence is presented in Fig. 3b to show its smooth decrease with distance. Locally the impact of anomalous propagation echoes reaches 60%, whereas the average is about 15%.

The hydrologically meaningful characterization of typical AP situations can be also expressed in terms of precipitation accumulation totals. Figure 4a shows an apparent cumulative rainfall map for the duration time of the 9/10 June superrefraction event, calculated from the 10-min lowest CAPPIs (constant-altitude plan position indicators) using the Marshall–Palmer Z–R relationship. For comparison the same is presented on Fig. 4b for heavy rainfall associated with a cold front that passed over Poland on 17 June 1991. The local accumulation maxima for the AP event are about four times higher than for the actual heavy rainfall. This demonstrates the crucial importance of the AP problem for hydrological applications of weather radar data.

3. Preparation of the calibration and validation samples

Data analyzed in this study come from an automated radar system located in the city of Legionowo near Warsaw, Poland. It is based on a non-Doppler, Russian-built MRL-5 radar with a 6-m-diameter antenna, having both S-band and X-band channels. Its signal processing unit does not contain any technical facilities for ground clutter or AP echo suppression. Permanent, near-the-radar ground clutter is effectively suppressed for X band by a software procedure. However, the procedure is not effective for S band (probably due to a very poor beam pattern for this channel), so operationally only X band is used. Because of this, our paper refers only to X-band data.

The system works 24 h per day performing a standard volume scan (14 elevations) every 10 min. The primary data are transformed from polar into rectan-
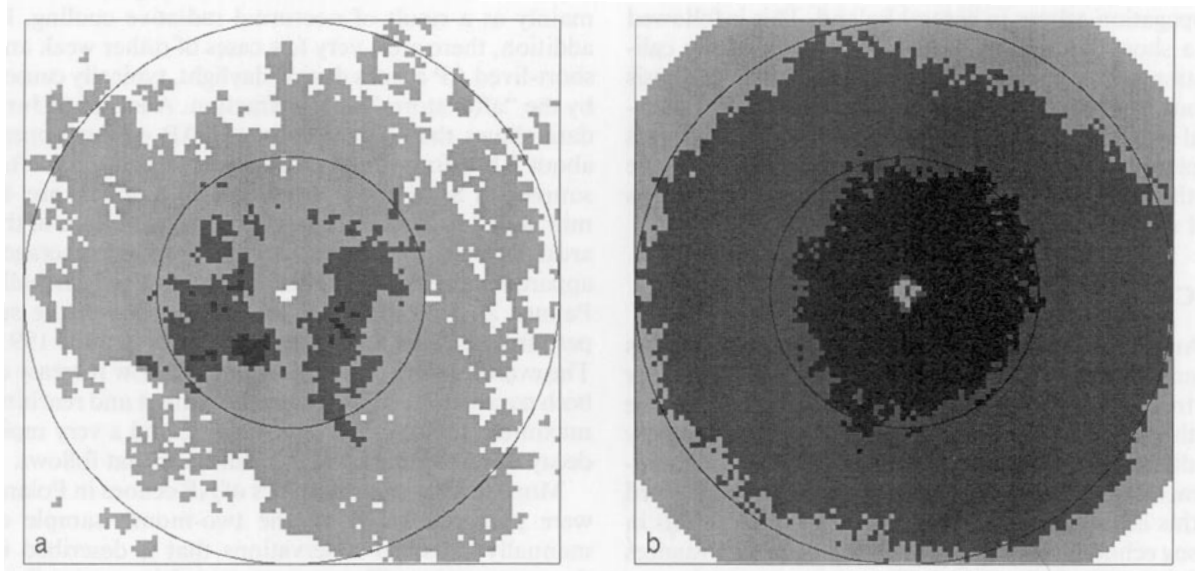

FIG. 3. Spatial distribution of (a) the conditional probability of AP echoes—the gray levels correspond to the following ranges: 0%–25%, 25%–50%, and above 50%; (b) probability of meteorological echo detection—the gray levels correspond to the following ranges: 0%–7%, 7%–14%, and above 14%. Both plots are based on a two-month sample of manually classified observations.
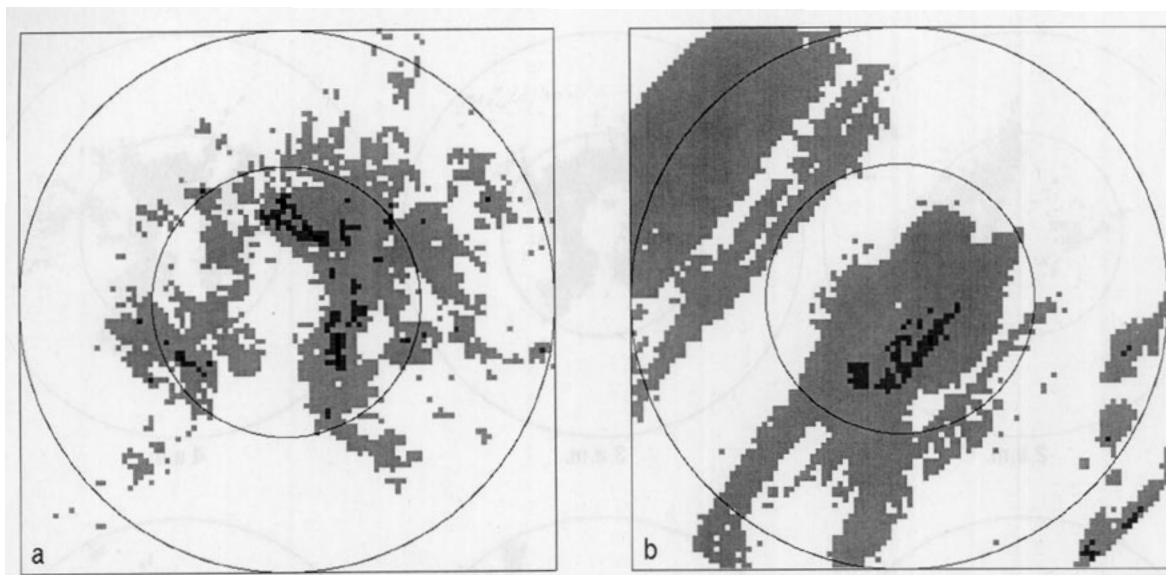
FIG. 4. Examples of storm-total rainfall accumulation maps calculated based on (a) the superrefraction situation of 10 June 1991—the gray levels correspond to the following ranges: 0–20, 20–40, and above 40 mm h^{-1}; (b) meteorological echo of 17 June 17 1991—the gray levels correspond to the following ranges: 0–10, 10–20, and above 20 mm h^{-1}. In both cases the Marshall–Palmer Z–R relationship was used.

gular coordinates. This results in several CAPPI radar reflectivity maps approximating horizontal cross sections of the atmosphere at predefined altitudes (0.7, 1, 2, 3, 4, and 5 km), and an echo tops map. These products have resolution of 4 km $\times$ 4 km and cover the area 400 km $\times$ 400 km around the radar site. The AP echo recognition map is an additional product obtained by the algorithm described in this study.

Data from June and September of 1991 were used—the June data as a calibration sample and the September data as an independent verification sample. Every observation used in this study was processed manually by an experienced meteorologist using specialized presentation and recording software. This resulted in truth maps of identified meteorological and AP echoes having the same format as the products mentioned above.

Reliable reference data sample is a crucial part of the AP recognition method, determining its practical effectiveness; therefore, much effort was put into its preparation. In classifying the echoes the operator took into consideration several characteristics of the radar echo pattern and the meteorological situation: the echo appearance and local morphology; the echo evolution and history using animation; the vertical echo structure; and the data from meteorological stations under the radar umbrella. Figure 5 shows a typical example of superrefraction associated with nocturnal radiative cooling during six consecutive hours on 9 and 10 June 1991. In spite of large variability in the echo pattern caused by the evolution of the inversion layer, and its short time fluctuations, characteristic morphological similarities are clearly visible.

As a result of manual recognition, we obtained a sample consisting of 631 166 data points with nonzero

classified echoes, 14.6% of them being AP echoes. The calibration sample (June 1991) contains 433 460 points (14.1% are AP), and the verification sample (September 1991) contains 197 706 points (15.7% are AP). A very small number of echoes (less than 0.5%), in regions where different echo types overlapped, could not be classified and were treated as undetermined; they were omitted during further data processing.

4. Echo-type recognition method

The theoretical basis for the discrimination function used in the AP detection algorithm is described in Duda and Hart (1973). To make the presentation in this paper self-contained, the main steps of the discrimination method are briefly repeated below.

Classification of the radar echoes into two classes ω_1 and ω_2 based on a feature vector $\mathbb{X}$ is based on the classical Bayes' formula

$$P(\omega_i \mid \mathbb{X}) = \frac{P(\mathbb{X} \mid \omega_i)P_i}{P(\mathbb{X})}, \qquad (1)$$

where $P(\ )$ denotes probability, $P(\ \mid\ )$ is conditional probability, and $P_i = P(\omega_i)$ is an a priori probability for class ω_i (of course $P_1 + P_2 = 1$). A decision rule assigning a particular echo to a given class is obtained by comparison of the conditional probabilities $P(\omega_1 \mid \mathbb{X})$ and $P(\omega_2 \mid \mathbb{X})$. This can be shown to be equivalent to comparing a discriminator function $G(\mathbb{X})$ against a given threshold. In our study we use the function $G(\mathbb{X})$ defined by

$$G(\mathbb{X}) = \ln\left[\frac{P(\omega_1 \mid \mathbb{X})}{P(\omega_2 \mid \mathbb{X})}\right]. \qquad (2)$$
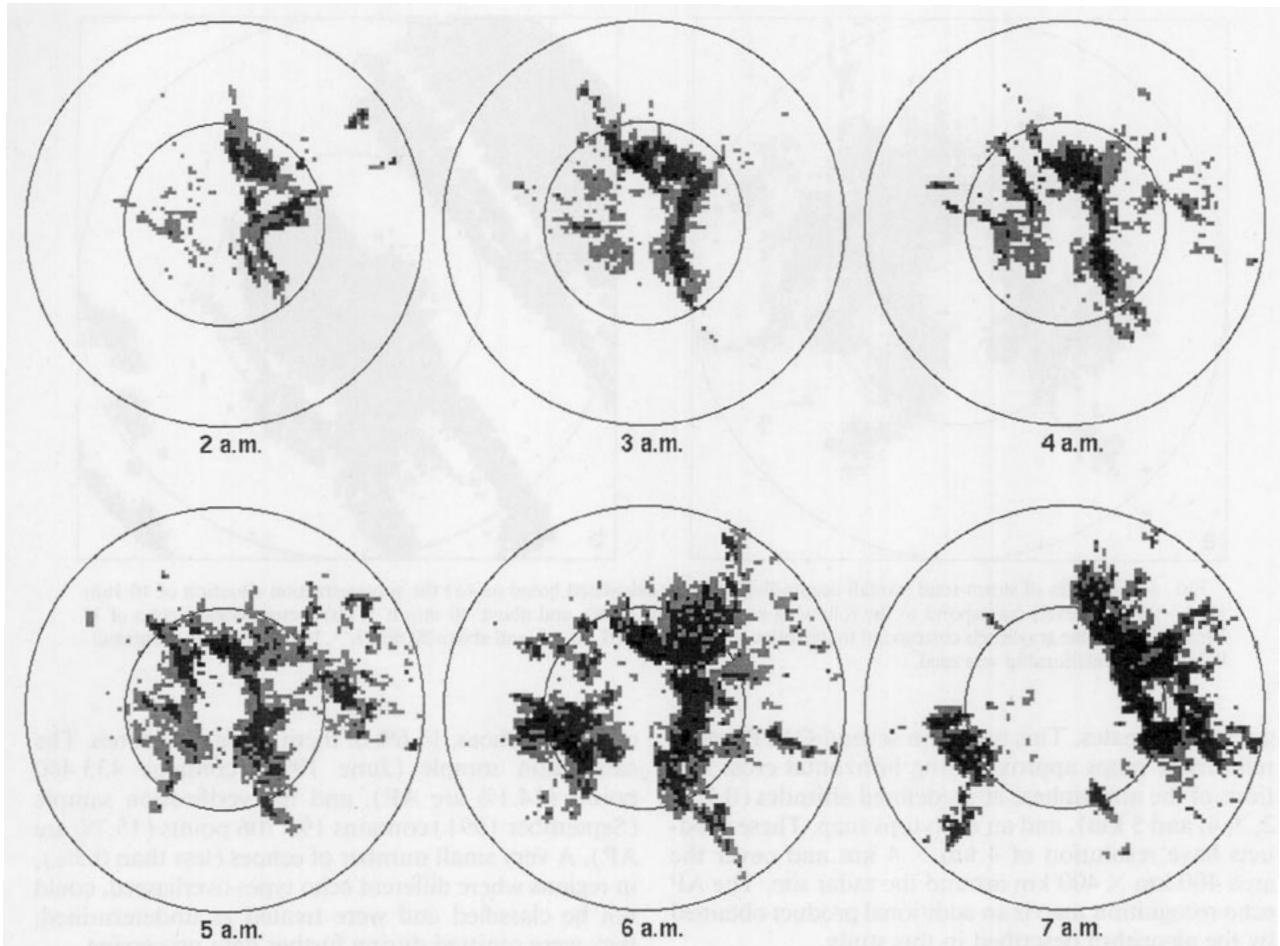
FIG. 5. Example of spatial pattern and time evolution of clear-air AP echoes caused by nocturnal radiative cooling on 10 June 1991. The maps are the 0.7-km-level CAPPIs. The range marks are at 100 km and 200 km; time is local. The gray levels correspond to the following ranges of radar reflectivity: 0–20, 20–40, and above 40 dBZ.

By assuming a zero threshold, we recognize a particular value of the feature vector as belonging to the ith class when conditional probability of the ith class is greater than the other. In this sense the above discrimination function performs echo recognition with minimal error; that is, the number of false recognitions in a large sample is minimal. In general, other optimization criteria for the recognition algorithm are possible, for example, minimization of the rainfall accumulation error using some simple Z–R transformation. However, the criterion used is the simplest one, and also has a big advantage of being the most universal, thus appealing to a broader class of users of radar data.

By substituting (1) we obtain the form

$$G(\mathbf{X}) = g_1(\mathbf{X}) - g_2(\mathbf{X}), \qquad (3)$$

where

$$g_i(\mathbf{X}) = \ln P(\mathbf{X}|\omega_i) + \ln P_i, \quad \text{for} \quad i = 1, 2. \quad (4)$$

In the study we assume that the conditional probabilities $P(\mathbf{X}|\omega_i)$ for $i = 1, 2$ are Gaussian distributed. In

our implementation of the method, this assumption is not exactly fulfilled. However, we used it to develop the AP discrimination formula, in order to take advantage of the simplicity of Gaussian formalism. We are aware that our approach is only a first approximation and the violation of the assumptions might influence the results significantly. However, the cross-validation technique used with independent verification samples gives us greater confidence in the results. We postponed the problem of finding the better method for future studies.

By assumption of Gaussian statistics the functions $g_i(\mathbf{X})$ take the form

$$g_i(\mathbf{X}) = -\frac{1}{2}(\mathbf{X} - \boldsymbol{\mu}_i)^{\mathrm{T}}(\Sigma_i)^{-1}(\mathbf{X} - \boldsymbol{\mu}_i)$$

$$-\frac{1}{2}\ln|\Sigma_i| + \ln P_i, \quad \text{for} \quad i = 1, 2, \quad (5)$$

where $\boldsymbol{\mu}_i$ is the expected value of the feature vector for the ith class, Σ_i is the covariance matrix for the ith class, and superscript T denotes matrix transpose.

Two cases can be distinguished. The case in which $\Sigma_1 \neq \Sigma_2$ leads to a quadratic discrimination function since both functions g_i in (3) are quadratic forms of a vector $\mathbf{X}$. We can simplify the problem significantly assuming $\Sigma_1 = \Sigma_2 = \Sigma$. Then, it can be shown that

$$G(\mathbf{X}) = [\Sigma^{-1}(\mu_1 - \mu_2)]^T(\mathbf{X} - \mathbf{X}_0), \quad (6)$$

where

$$\mathbf{X}_0 = \frac{1}{2}(\mu_1 - \mu_2) - \frac{\ln(P_1/P_2)(\mu_1 - \mu_2)}{(\mu_1 - \mu_2)^T \Sigma^{-1}(\mu_1 - \mu_2)}. \quad (7)$$

The difference between the quadratic and linear discrimination functions should be analyzed in both geometric and statistical terms. In the linear case the boundary separating the classes in the parameter space is a linear subspace (hyperplane), whereas in the quadratic case it is curvilinear and thus allows for more subtle discrimination. However, the number of parameters to be estimated and subsequently their estimate uncertainties in the nonlinear case are much greater (two covariance matrices) than for the linear discriminator. So, even if the assumption of equal covariance matrices in not exactly true, the performance of the linear discrimination function must not necessarily be worse.

5. Implementation of the recognition method

Implementation of the statistical method proposed in the previous chapter to detect anomalous propagation echoes includes two major steps: choice of the parameters describing the echo to build the feature vector $\mathbf{X}$, and estimation of the coefficients of the discrimination function used.

The feature vector is based on analysis of the maps of radar products described in section 3. Sets of up to five parameters derived from the maps were selected and organized into the vector $\mathbf{x} = (x_1, x_2, \cdots, x_n)$. The vector was calculated at each location u_{ij} of the grid for which nonzero radar echo was recorded. The chosen parameters have the following meaning. Parameter x_1 is defined as

$$x_1 = 200 \sin\alpha, \quad (8)$$

where α is the elevation angle that corresponds to the highest nonzero reflectivity level at the location u_{ij}. The coefficient 200 plays the role of just a scaling factor, introduced to obtain similar magnitude orders of all parameters. Parameter x_2 is calculated as

$$x_2 = 200 \sin\alpha_{max}, \quad (9)$$

where α_{max} is the angle corresponding to the level of maximum reflectivity at the u_{ij}. Parameter x_3 is simply the maximum reflectivity calculated at location u_{ij}, chosen from all the available CAPPIs. It is expressed in units of one-third of dBZ. Parameter x_4 is the maximum difference between the value of x_3 at location u_{ij} and its immediate neighbors, characterizing the local gradients of the echo pattern. If any of the neighboring values is zero, parameter x_4 takes on the value of x_3. Finally, parameter x_5 is the echo top expressed in units of 0.1 km.

In the present study the choice of the discrimination parameters creating the feature vector was intuitive and subjective. No objective selection or comparison procedure was applied, and we consider it as a subject for future investigation. The manual preparation of the data sample described in section 3 provided the experience and intuitive background to find the echo parameters that seemed to us the best for the feature vector used in the AP recognition algorithm. Parameter x_4 (local gradients) attempts to describe differences in the local morphological structure of the meteorological and AP patterns. Parameters x_1 and x_2 try to take into account the apparent increase of the height of the AP echo features with distance by applying the elevation angle. Other factors were also considered—parameters x_3 and x_5 are just standard predictors used in our operational service.

It is often believed that quantitative characteristics of temporal changes of radar image should be a powerful discriminating factor for AP detection. As a matter of fact, animation was a very powerful tool in the subjective classification of the radar echoes by a human operator. However, in the present work we did not include such characteristics in the feature vector. One reason is difficulty in mathematical formulation of the proper parameterization. In the subjective analysis, the several hours "life history" of the echo was very meaningful. The characteristics of an instantaneous echo motion, which are much easier to formalize, proved to be misleading in many situations.

Analysis of the calibration sample of the June echoes allowed us to estimate the coefficients of the discrimination functions described in section 4. For example, the estimates of the mean vectors in the two classes are as follows: for the meteorological echo $\mu_1 = (6.26, 1.57, 66.75, 26.47, 51.53)$, for the AP echo $\mu_2 = (4.69, 0.15, 58.37, 44.32, 16.55)$.

It can be seen, that except for x_3 (maximal reflectivity factor) and x_1 (the angular height of the echo), the differences between μ_1 and μ_2 are quite large, which indicates that the chosen parameters could be adequate for the recognition of the analyzed echo types. The local gradients are much bigger for the AP than for the meteorological echoes. The echo tops and the elevations of the maximum reflectivity are much lower for the AP than for the meteorological echoes. For comparison, three types of discrimination functions were analyzed: with all five parameters, with four parameters (without x_3), and with three parameters (without x_1 and x_3). They were calculated for both the linear and quadratic case. As an example we present the estimated forms of the linear discrimination functions: G_5, G_4, and G_3 for five, four, and three parameters, respectively:

TABLE 1. Absolute and relative errors of radar echo-type recognition with three linear discrimination functions for the calibration sample of June. The errors are given separately for three classes of echo: only meteorological, only AP, and both meteorological and AP.

Discrimination function	Echo type	Number of points	Number of errors	Percentage of errors
G_5	meteorological	372 364	5698	1.53
	AP	61 096	9596	15.71
	meteorological + AP	433 460	15 294	3.53
G_4	meteorological	372 364	4732	1.27
	AP	61 096	10 737	17.57
	meteorological + AP	433 460	15 469	3.57
G_3	meteorological	372 364	3816	1.02
	AP	61 096	13 021	21.31
	meteorological + AP	433 460	16 837	3.88

$$G_5 = -0.18x_1 + 0.38x_2 - 0.0045x_3$$
$$- 0.064x_4 + 0.17x_5 - 2.5 + \beta, \quad (10)$$
$$G_4 = -0.18x_1 + 0.38x_2 - 0.058x_4$$
$$+ 0.265x_5 - 2.7 + \beta, \quad (11)$$
$$G_3 = -0.018x_2 - 0.0725x_4 + 0.136x_5 - 2.04 + \beta, \quad (12)$$

where $\beta = \ln P_1 - \ln P_2 = \ln(1 - P_2) - \ln P_2$.

The total number of meteorological (rain) echoes in the June sample amounted to 372 364 and that of AP echoes to 61 096. Thus the estimates of the a priori probabilities for the June sample are $P_1 = 0.86$ and $P_2 = 0.14$, and $\beta = 1.81$. The discrimination process consists in comparing the value of the function with zero threshold. For example $G_5(\mathbf{X} = \mu_1) = 5.55 > 0$, and $G_5(\mathbf{X} = \mu_2) = -1.76 < 0$. So points with feature vectors similar to μ_2 will be classified as AP echoes, whereas points with feature vectors similar to μ_1 will be classified as meteorological echoes.

6. Results

The performance of the echo-type recognition by the discrimination functions (10), (11), and (12) and

their quadratic five-, four-, and three-predictor versions are presented in Tables 1–3. The classification errors are given both in terms of the number of erroneously recognized grid points and their percentages for both types of echo, together and separately, for meteorological echoes (points recognized as AP) and anomalous clutter echoes (points recognized as meteorological).

The scores of the echo-type recognition by linear discrimination functions (10), (11), and (12) on the calibration sample of June 1991 are presented in Table 1. It can be seen that the four-parameter function G_4 [Eq. (11)] gives virtually the same results as the five-parameter function G_5 [Eq. (10)]. The three-parameter function G_3 [Eq. (12)] gives slightly worse results. For all three functions the general classification error is of the order of 4%, and the errors in the class of AP echoes are much larger than in the meteorological class.

The independent verification of the echo-type recognition by the same linear discrimination functions (10), (11), and (12) on the validation sample of September 1991 is given in Table 2. In this case the general recognition error ranges from 5.3% to 5.8%. The performance is only slightly worse than for the calibration sample on which the function coefficients were fitted. This shows that the algorithm is statistically stable and may be applied to new observations and different sea-

TABLE 2. Absolute and relative errors of radar echo-type recognition with three linear discrimination functions for the verification sample of September. The errors are given separately for three classes of echo: only meteorological, only AP, and both meteorological and AP.

Discrimination function	Echo type	Number of points	Number of errors	Percentage of errors
G_5	meteorological	166 733	7718	4.63
	AP	30 973	3775	12.19
	meteorological + AP	197 706	11 493	5.81
G_4	meteorological	166 733	1046	0.63
	AP	30 973	10 222	33.00
	meteorological + AP	197 706	11 268	5.70
G_3	meteorological	166 733	5354	3.21
	AP	30 973	5198	16.78
	meteorological + AP	197 706	10 552	5.34

TABLE 3. Absolute and relative errors of radar echo-type recognition with three quadratic discrimination functions for the calibration sample of June. The errors are given separately for three classes of echo: only meteorological, only AP, and both meteorological and AP.

Discrimination function	Echo type	Number of points	Number of errors	Percentage of errors
Five-parameter function	meteorological	372 364	26 773	7.19
	AP	61 096	4533	7.42
	meteorological + AP	433 460	31 306	7.22
Four-parameter function	meteorological	372 364	28 970	7.78
	AP	61 096	4546	7.44
	meteorological + AP	433 460	33 516	7.73
Three-parameter function	meteorological	372 364	16 868	4.53
	AP	61 096	5230	8.56
	meteorological + AP	433 460	22 098	5.10

sons. The three-parameter function G_3 gives better results than functions G_4 and G_5. This indicates that parameters x_1 (elevation of echo top) and x_3 (maximum reflectivity) do not add significant information to the three best parameters chosen.

The errors of the echo-type recognition by three nonlinear discrimination functions (five, four, and three predictors) for the calibration sample of June 1991 are presented in Table 3. This version of the method does not assume equal covariance matrices for the two classes of the radar echo. It can be seen that the overall errors for all three quadratic functions are bigger than for their equivalent (in predictor choice) linear versions. For that reason the linear discrimination function was used in the subsequent analysis.

The performance evaluation in terms of recognition error is not the best one from the hydrological point of view. If the radar is to be used for quantitative estimation of rainfall, the errors in estimating rain totals are more meaningful. The rain monthly (for both the June and September samples) totals were calculated for the following cases:

1) the "true" totals calculated only for the meteorological (manually recognized) echoes;
2) the totals without any AP echo elimination;
3) the totals with AP echo elimination using the linear discrimination function G_5.

In all cases the calculations of the rainfall intensities were based on the lowest CAPPI. The conversion from the radar reflectivities was done using the standard Marshall–Palmer Z–R relationship.

Table 4 presents the monthly totals and the corresponding errors for the above cases. The impact of the unsuppressed AP echoes on the monthly accumulated precipitation is 59% of the actual sum for the month of June and as much as 97% for September. Applying our AP elimination method in the linear five-parameter version reduces the monthly total error to −3.4% for June and to −11.8% for September. The relative errors of rain totals are much higher for September than for June, but the September total is much smaller than that of June, and the absolute errors are of comparable magnitude.

7. Conclusions

These preliminary results show that application of the linear discrimination functions permits classification of radar echoes into AP and meteorological echoes. The level of total error of recognition is on the order of some 4% for the calibration sample, and about 6% for the independent verification sample. After the AP elimination, the bias of monthly rainfall total is on the order of −4% for the calibration sample and −12% for the verification sample. This is a tremendous improvement in comparison with the rainfall overestimation obtained without any AP suppression. Application of quadratic discrimination functions failed to improve the recognition. This can be attributed to the violation

TABLE 4. Monthly rain totals and the corresponding errors without AP echo elimination and with automatic elimination based on linear discrimination function G_5. The first row gives the "true" monthly total based on manual echo-type recognition.

	June			September		
Case	Total (mm)	Error (mm)	Error (%)	Total (mm)	Error (mm)	Error (%)
Meteorological echo	219.0			47.8		
Without AP elimination	348.7	+129.7	+59.2	94.3	+46.5	+97.3
After elimination by linear G_5	211.5	−7.5	−3.4	42.2	−5.6	−11.8

of the assumption of normality of the predictors joint distribution. It is very likely that for the nonlinear version of the method this assumption is more critical.

The experimental and software framework established to perform this study, as well as the experience gained, create an excellent basis for further systematic investigation of the AP suppression problem. We will test modifications of the recognition method that would allow us to relax its assumptions and to apply more sophisticated versions of the discrimination function. The next problem to investigate should be systematic verification of different echo parameters used in the feature vector. Quantitative characteristics of the horizontal and vertical structure of the radar echo pattern seem to be the most promising. Also it is believed that by collecting a larger calibration sample, allowing statistically improved estimation of the algorithm coefficients, we will obtain better performance of AP echo detection than our preliminary results.

The applicability of the discrimination functions presented in section 5 is limited to one radar band and one climatic regime. However, our method can be expanded to other radar installations by recalibration of the function coefficients. Also, for multiparameter radar, echo features other than those based on radar reflectivity only can be utilized. The reported results should be viewed as an example of one method and its performance rather than a comprehensive evaluation of the statistical methods of AP removal.

From the point of view of operational implementation in hydrometeorological service, the described method is just one element in a system of radar-based forecasting and analysis. It should be viewed as a tool helping, but not replacing, the operator skills and experience. The method presented here is flexible; for example, the a priori probability P_2 (or alternatively P_1) determines the location of the discrimination surface in the parameter space. It can be determined as a constant based on the data sample (as in our study), or treated as an operational parameter to adjust the algorithm to the preference of a user. By manipulating this coefficient an operator can amplify or attenuate the AP elimination.

REFERENCES

Battan, L. J., 1973: *Radar Observation of the Atmosphere.* University of Chicago Press, 324 pp.

Bean, B. R., and E. J. Dutton, 1968: *Radio Meteorology.* Dover, 417 pp.

Duda, R. O., and P. E. Hart, 1973: *Pattern Classification and Scene Analysis.* Wiley-Interscience, 386 pp.

Doviak, R. J., and D. S. Zrnić, 1984: *Doppler Radar and Weather Observations.* Academic Press, 458 pp.

Fiore, J. V., Jr., R. K. Farnsworth, and G. Huffman, 1986: Quality control of radar-rainfall data with VISSR satellite data. Preprints, *23d Conf. on Radar Meteorology and Cloud Physics,* Snowmass, CO, Amer. Meteor. Soc., JP15–JP19.

Hamuzu, K., and M. Wakabayashi, 1991: Ground clutter rejection for weather radar and weather Doppler radar. *Hydrological Applications of Weather Radar,* Cluckie and Collier, Eds., Ellis Horwood Ltd., 131–142.

Ko, H., 1985: A practical guide to anomalous propagation. *Microwaves and Rf,* 71–76.